Effect of massive outer leaf of an insulated cavity brick wall on heat loss

R. Lindberg [a], J. Rantala [a], V. Leivo[a] , M. Kiviste [a]
[a] Department of Civil Engineering, Tampere University of Technology, P.O. Box 600, FI-33101 Tampere, Finland

Abstract

The availability of coherent long-term measured data on climatic variables and building parameters forms the basis for predicting, analyzing and simulating the heating or cooling energy demand on buildings. This paper analyses measured four year data considering the test building with an insulated cavity brick wall with a massive outer brick leaf. The results show that the solar radiation and the thermal inertia of massive outer leaf of a wall have a significant effect on the heat loss and energy consumption of the buildings throughout the Finland and Scandinavia. Based on average outdoor air temperatures, the nominal calculated heat losses could be over-estimated. For more accurate heat losses the outdoor surface temperature should be applied as a boundary condition.
The measure results were verified with finite element method.

Keywords: Thermal performance, thermal inertia, heat loss, external wall, measured data

Introduction

There is a growing interest towards energy saving and efficiency of buildings. It has been noticed that besides the U-value, the thermal inertia should also be considered in energy conscious building design. The influence of the thermal inertia of building structures on thermal comfort and energy consumption has been analysed theoretically (Guglielmini et al., 1981). Also, the combined effect of thermal inertia and surface absorptance for solar radiation of external walls on the thermal behavior of buildings was calculated in unsteady state conditions (Guglielmini et al., 1982). Thermal inertia has found to be an important parameter for improving thermal comfort as well as for reducing heating and cooling energy consumption of buildings (Feng, 2004; Balaras, 1996). The influence of thermal inertia of Spanish (Oroza and Oliveira, 2012) and Italian (Di Perna et al., 2011) school building envelope on indoor environment has been studied. The problem of the room temperature oscillation under intermittent heating and solar radiation was analysed for two types of composite walls which have the same the same U-value and different heat capacities (Faggiani et al., 1984). The thermal inertia of external walls with the same *U*-value is also compared in order to evaluate the influence of the relative position of a given thickness of insulation and a massive layer (Kossecka and Kosny, 2002; Bojic and Loveday, 1997). Several external wall systems with the same U-value but different dynamic properties are analysed in order to calculate the associated achievable energy savings (Aste et al., 2009). However, the results regarding the energy saving potential of thermal inertia are ranging from a few percentages to more than 80% (Kossecka and Kosny, 2002; Bojic and Loveday, 1997). The differences in input data cause often greater differences in calculation results than the differences between various calculation and simulation methods (Kalema et al., 2008).

The availability of coherent long-term measured data on climatic variables and building parameters forms the basis for predicting, analysing and simulating the heating or cooling energy demand of buildings. The accurate prediction requires detailed input data and understanding of time-dependent temperature distribution within the external wall structures. However, that kind of data is still scarce in literature.

This paper considers the results of a four year long field survey, where the thermal performance of external walls of eight identical tests buildings were monitored constantly throughout the year

(Lindberg et al., 2004). Each building had exterior wall constructed of different building materials. The data considered the indoor-outdoor temperatures, temperatures at various depths within the northern, southern and western exterior wall facades, the wind speed and direction as well as the horizontal global solar radiation. A computer system was used to monitor, check, calculate, integrate and save the data acquired from approximately 520 sensors in each building. Measurements were taken with a time interval of 20 seconds. These values were integrated over a time interval of 30 minutes and the minimum, maximum and mean values were subsequently stored to a computer database.

Many structural solutions of external walls include an external leaf outside the thin air gap made of some durable bulky material with a considerable thermal inertia, such as brickwork or concrete. The gathered data considering the test building with an insulated cavity brick wall as an external wall envelope is further analysed in this paper. The details of the exterior wall structure with the corresponding material parameters are presented in Fig. 1 and Table 1. Finite element method (FEM) was applied to verify the measured thermal behavior of the wall structure.

Methodology

The test building

The floor area of each test building is 2.4 m × 2.4 m and the free floor to ceiling height 2.6 m. Buildings were constructed in a moderately exposed parking area within the compound of Tampere University of Technology. They were oriented in north-south direction is such a way that the external doors of each building are installed within the eastern wall. There are no other openings or windows in the external walls. The ceilings and the floors of all the buildings are equally composed of two layers of foamed polyurethane elements with an overall thickness of 200 mm. The joints between the insulation elements were sealed with polyurethane foam and ventilation tapes. The test building was heated with a 1500 W electric radiator (1248 mm × 400 mm heat panel) (Table 1).More detailed description of all the eight test buildings is available in the paper by Lindberg et al. (2004). Fig. 1. and Table 2 present the structural layout and the materials of the insulated cavity brick wall.

Data collection

Prevailing weather conditions were measured at the site, including the outdoor temperatures, wind speed and direction, and the relative humidity of the air. The intensity of the solar radiation was also measured by a pyranometer (solar meter) that was fixed on the eaves level of one of the test buildings. The pyranometer measured the global solar radiation to the building surface, which is composed of the direct and the diffused solar radiation.

The indoor air temperature was monitored at three heights (near the floor surface, at the middle and near the ceiling). Temperatures inside the wall cross-section were monitored in 14 different levels, including the inner and outer surfaces of the wall. Calibrated semi-conductor sensors were used as the measuring devices. The same kind of test setting was implemented inside the three solid walls of the building facing south, west and north. The location of the individual temperature gauges inside the wall structure is illustrated in Fig. 2.

Multiplexers were used to collect the data from the sensors so that the readings from each channel (temperature gauge) were recorded to a computer every 20 seconds. Analog-to-Digital and Digital-to-Analog (ADDA) cards were use for data collection and conversion. The mean temperatures from the 20s measured values were saved to a computer hard disc every 30 minutes.

Measurement data

Temperature distribution

Measured temperature distribution inside the wall section is here considered during a representative period of the survey in late February 2005 only. The aim was to illustrate the effect of a massive outer leaf of a wall on thermal loss through the entire structure. The monthly heat loss calculus is performed for the entire survey period between 2002 and 2006.

Fig. 3 illustrates the dependency between the surface temperature of the external brick leaf of the wall and the measured solar radiation at the site during late February 2005. Correlation between the measured solar irradiation at the site and the measured surface temperature of the brickwork is evident. The average ambient outdoor temperature during the period was $T_{out,ave}$ = -9.3° C, as the average surface temperature during the same period was $T_{surf,ave}$ = -5.2° C, which is 44 % less than outdoor temperature.

Fig. 4 shows the measured temperature distribution inside the wall structure during a 24 hrs period in 27th of February 2005. The maximum measured outdoor temperature of the day was $T_{out,max}$ = -6.4° C at 15:02 hrs (Fig. 4). Meanwhile the measured surface temperature of the outer brick leaf (point 395, Fig. 2) was $T_{surf(395)}$ = +17.9° C (15:02 hrs, Fig. 4) and the temperature of the inner surface of the brick leaf $T_{surf(310)}$ = +14.7° C. Temperature difference between the ambient air and inner brick surface (point 310, Fig. 2) was ΔT = 21.1° C. This temperature difference between the ambient outdoor air and the inner surface of the face brick leaf generated by solar radiation has a significant effect on the actual heat loss through the insulation layer, as shown in measured temperature distribution curves (Fig. 4).

Due to the high thermal inertia of the brick leaf temperature of the inner surface of the leaf facing the air gap remains relatively high until early evening though the outer surface temperature of the leaf had already decreased significantly. At 21:00 hrs, the measured ambient outdoor temperature was T_{out} = -13.1° C, temperature of the outer surface of the brick leaf $T_{surf(395)}$ = -7.5° C and the measured temperature of the inner surface of the leaf $T_{surf(310)}$ = -3.6° C. The difference between the surface facing the air gap and the ambient air was still ΔT = 9.5° C.

Heat flow through the wall

Heat flow through the wall or any individual material layer was calculated according to the standard EN ISO 6946 (2007). Two different methods were used:

1) The nominal heat loss was determined based on the ambient average outdoor and indoor temperatures, measured every half hour at the site, and the total thermal resistance of the entire wall structure, including the inner and outer surface resistances and the thermal resistance of the air gap and the outer brick leaf according to guidance given to the unventilated air layers in EN ISO 6946 (2007). The standard concludes that the open vertical joints in the outer leaf of a masonry cavity are not regarded as ventilation openings. Thermal transmittance of the entire wall used in calculations is given in Table 1 (U_{wall} = 0.25 W/m^{2}K). This method is widely used in Finnish codes, for example in calculation of the heat loss energies through the exterior walls when the required heating capacity or the energy consumption of a building is determined.

2) The second method applied the measured temperatures inside the wall structure, recorded similarly every 30 minutes during the entire survey period. This actual heat loss from the building was determined from the measured temperature difference over the d = 125 mm thick mineral wool

layer outside the inner brick wall. This way the thermal inertia of the inner brick layer does not have an effect on the readings, and the flow through the insulation layer denotes the actual heat loss from the indoor air and the inner surface of the external wall. Only the nominal thermal conductivity of the mineral wool ($\lambda_{U,min.wool}$ = 0.045 W/m^{2}K) was used when thermal transmittance of the layer was determined ($U_{min.wool}$ = 0.36 W/m^{2}K). Now the daily fluctuation of temperature and thermal inertia of the outer brick leaf have a significant effect on the calculated heat flow through the insulation layer.

Table 3 shows the heat loss through the external wall per a square meter, determined from the measured temperature levels inside the wall structure, and the measured temperatures of the outdoor and indoor air. Both calculation methods described earlier were used. The heat loss was calculated in 30 minute intervals and summed up as a monthly heat loss Φ_m [kWh/m^2].

The heating season was determined from the indoor air temperature data (Fig. 5). The additional heating was required to keep the temperature at the required T_{indoor} ≈+19° C between late September and late April. The heating season therefore included the seven months between October and April.

Fig. 6 illustrates the difference between the actual measured heat loss through the wall section and the nominal loss calculated from the ambient outdoor and indoor temperatures (Δ%). The difference is most significant during the spring on the South facing wall, starting from the late February and lasting until the end of the heating season in April. The actual heat loss in February was over 10 % less than the nominal loss due to the increased solar radiation towards the end of the month. In March the difference was already between 18… 27 %, and in April between 32…55 %. In autumn a significant difference was measured in early October, the monthly difference varying between 9…20 % , which rapidly decreased towards the end of the year, being less than 5 % during the three winter months between November – January.

The measured heat loss difference during the entire heating season varied between 11…23 % in the four year survey period. Only during the three darkest winter months (November-January) the measured heat flux more or less equals the nominal heat loss calculated from the ambient indoor and outdoor temperatures. From May onwards the measured temperatures inside the test building rose above the limit value of T_{indoor} = +19° C, the additional heating was no longer needed and the measured heat flow rate through the wall (Table 3) is due to the risen average indoor air temperatures. Instead of heating, a cooling system of some kind would have been needed, especially in July and August while the average indoor air temperature rose above +25° C degrees, despite the fact that the test building had not any window openings to let the solar radiation in.

The measured difference between the actual and the nominal heat loss is less dramatic, but still significant on the North facing wall. The difference during the spring months varied between 12…18 % in April, and between 7…10 % in March. In autumn the difference was less dramatic. In October it was between 0…10 % , and usually less than 5 % during the following three winter months.

FE modeling and verification of the measurement data

Finite element method was used to verify the measured thermal behavior of the wall structure. Two-dimensional FE –model included a one meter high section of the wall structure. The measured indoor air temperature was given as the inner boundary condition for the model with a constant surface resistance (R_{si} = 0.13 m^2·K/W) applied on the inner surface of the wall. The required thermal coefficients of the materials applied in the analysis are presented in Table 1.

The exact solar radiation rates or wind conditions at the instant vicinity of the surveyed walls were not known (only ambient conditions at the site were measured). Therefore the measured surface temperature of the outer brick leaf was used as the outdoors boundary condition. It was applied as a thermal load directly on the outer surface of the brickwork. Thermal interaction over the air gap was calculated using the surface to surface radiation and conductance, with up flowing heat flow inside the gap dependent on the temperature of the brickwork. Increasing surface temperature of the brickwork increases the air velocity inside the cavity due to the increased temperature difference between the air gap air and the ambient outdoor air.

Fig. 7 illustrates the measured and calculated temperatures at three points inside the wall structure. The given number denotes the distance from the inner surface of the wall structure. Thus, the point 135 denotes the outer surface of the load bearing brick wall (Fig. 2), point 260 is the joint surface between the mineral wool and the wind shield board, and 310 is the surface of the brickwork facing the air gap. The other curves in Fig. 7; the measured indoor air temperature and the wall surface which denotes the measured outer surface temperature of the brickwork, were both used as the given boundary conditions in calculus (Fig. 2).

Correspondences between the measured and calculated values were good as far as the temperature distribution inside the wall structure was considered. Also the calculated heat flux through the mineral wall layer (FEM, Fig. 8) equaled the flux determined from the measured boundary temperatures of the layer (Measured, Fig. 8). The cumulative difference between the two fluxes during the 2-day period was only 1.4 %. The FE –analysis verified the in-situ measurements and proved the effect of the thermal inertia of the faced brickwork on the actual heat loss through the wall. Flux curves in Fig. 7 show how the temperature increase of the outer brick leaf during the day (between noon and 9 pm) decreases the actual heat loss by 25 % in comparison to the reference flux (Reference, Fig. 8) calculated using the total thermal resistance of the wall and the measured ambient outdoor and indoor temperatures.

It can be found from current study that differences in average outdoor air and outdoor surface temperatures (Fig. 4) will result in considerable differences in heat fluxes (Fig. 8) and heat losses (Fig. 6). Based on average outdoor air temperatures, the heat losses of external walls of a building cannot be calculated accurately. This way the heat losses could be over-estimated. Therefore, outdoor surface temperature is a very important boundary condition in order to calculate accurate heat losses of a building.

Conclusions

Thermal inertia of the massive outer leaf of an insulated cavity brick wall has a significant impact on heat flow through the wall. Solar radiation heats up the outer leaf in comparison to the ambient outdoor air temperature surrounding the building. Due to the thermal inertia of the leaf, the temperature difference between the leaf and the outdoor air remains significantly high until late evening.

On the South facing wall this thermal fluctuation of the massive outer leaf of the wall has a significant effect on the total thermal loss through the structure. According to the four year measurement data the heating season of the test building lasted seven months from early October to late April. Only during the three darkest winter months (November-January) the nominal calculated heat loss corresponded relatively well with the measured losses. In October and between mid-February and April the solar radiation had a significant effect on the measured heat loss. The actual heat loss in February was over 10 % less than the nominal loss due to the increased solar radiation towards the end of the month. In March the difference was already between 18… 27 %,

and in April between 32…55 %. In autumn a significant difference was measured in early October, the monthly difference varying between 9…20 %, which rapidly decreased towards the end of the year. Overall the difference between the measured and nominal loss during the heating season varied between 11…23 % in the four year survey period.

On the North facing wall the measured difference between the actual and the nominal heat loss is less dramatic, but still significant. The difference during the spring months varied between 12…18 % in April, and between 7…10 % in March. In autumn the difference was less dramatic. In October it was between 0…10 %, and usually less than 5 % during the following three winter months. The results of current study show that the nominal calculated heat losses, based on average outdoor air temperature, could be over-estimated. For more accurate heat losses the outdoor surface temperature should be applied as a boundary condition.

The northern location (latitude 61°25' N) of the survey site suggests, that the solar radiation and the thermal inertia of the different structural sections of a wall have a significant effect on the actual heat loss and energy consumption of the buildings throughout the Finland and Scandinavia, as the average solar irradiation increases toward the South and most of the Scandinavian building stock is located South from the survey site. Nowadays the structural solutions of the Finnish external walls are designed considering only three or four months of the year, from November to early February, and the nominal theoretical heat loss through the wall during this period. In order to improve the energy efficiency of the building envelope, thermal insulation capacity of the wall is increased and will be further increased in the future. The basic idea is to reduce the heat loss and energy consumption of the building by 20 % by increasing the thermal insulation capacity of the wall by that same amount, 20 %. This highly theoretical approach only considers the three winter months of the year and ignores the other possibilities to improve overall thermal behavior of the wall, not to mention the five summer months during which the additional heating is usually not needed at all, but a cooling system is almost a necessity.

References

Aste N, Angelotti A and Buzzetti M (2009) The influence of the external walls thermal inertia on the energy performance of well insulated buildings. *Energy and Buildings* 41: 1181-1187.

Balaras CA (1996) The role of thermal mass on the cooling load of buildings: an overview of computational methods. *Energy and Buildings* 24: 1–10.

Bojic M and Loveday DL (1997) The influence on building thermal behavior of the insulation/masonry distribution in a three-layered construction. *Energy and Buildings* 26: 153–157.

Di Perna C, Stazi F, Ursini Casalena A and D'Orazio M (2011) Influence of the internal inertia of the building envelope on summertime comfort in buildings with high internal heat loads. *Energy and Buildings* 43: 200-206.

EN ISO 6946 (2007) Building components and building elements – Thermal resistance and thermal transmittance – Calculation method.

Faggiani S, Galbiati P and Tuoni G (1984) Thermal behavior of composite walls under solar irradiation and internal intermittent heating. *Journal of Building Physics* 7: 202-213.

Feng Y (2004) Thermal design standards for energy efficiency of residential buildings in hot summer/cold winter zones. *Energy and Buildings* 36: 1309–1312.

Guglielmini G, Magrini U and Nannei E (1981) The influence of the thermal inertia of building structures on comfort and energy consumption. *Journal of Building Physics* 5: 59-72.

Guglielmini G, Magrini U and Nannei E (1982) Heat transmission in buildings: combined effect of absorptance and thermal inertia of exterior walls. *Journal of Building Physics* 6: 3-13.

Kalema T, Johannesson G, Pylsy P, Hagengran P (2008) Accuracy of energy analysis of buildings: A comparison of a monthly energy balance method and simulation methods in calculating the energy consumption and the effect of thermal mass. *Journal of Building Physics* 32: 101-130.

Kossecka E and Kosny J (2002) Influence of insulation configuration on heating and cooling loads in a continuously used building. *Energy and Buildings* 34: 321–331.

Lindberg R, Binamu A and Teikari M (2004) Five-year data of measured weather, energy consumption, and time-dependent temperature variations within different exterior wall structures. *Energy and Buildings* 36: 495-501.

Orosa JA and Oliveira AC (2012) A field study on building inertia and its effects on indoor thermal environment. *Renewable Energy* 37: 89-96.

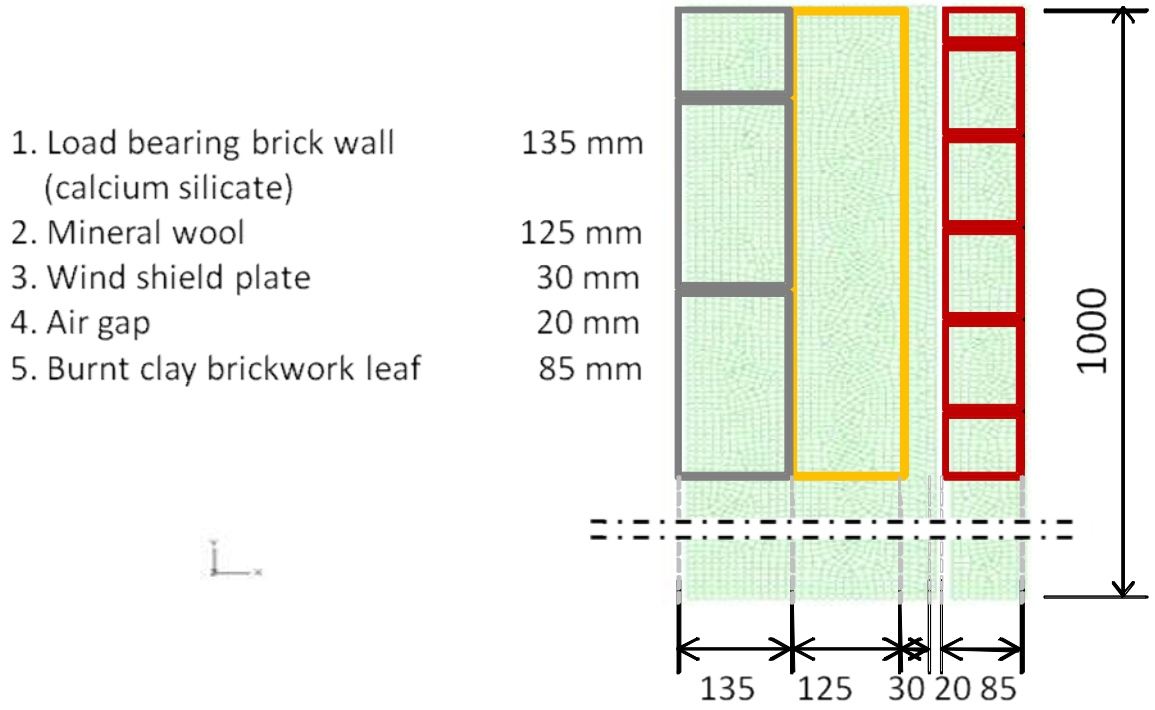

Fig. 1. Structural details of the insulated cavity brick wall, and the 2D FE-mesh applied in the verification.

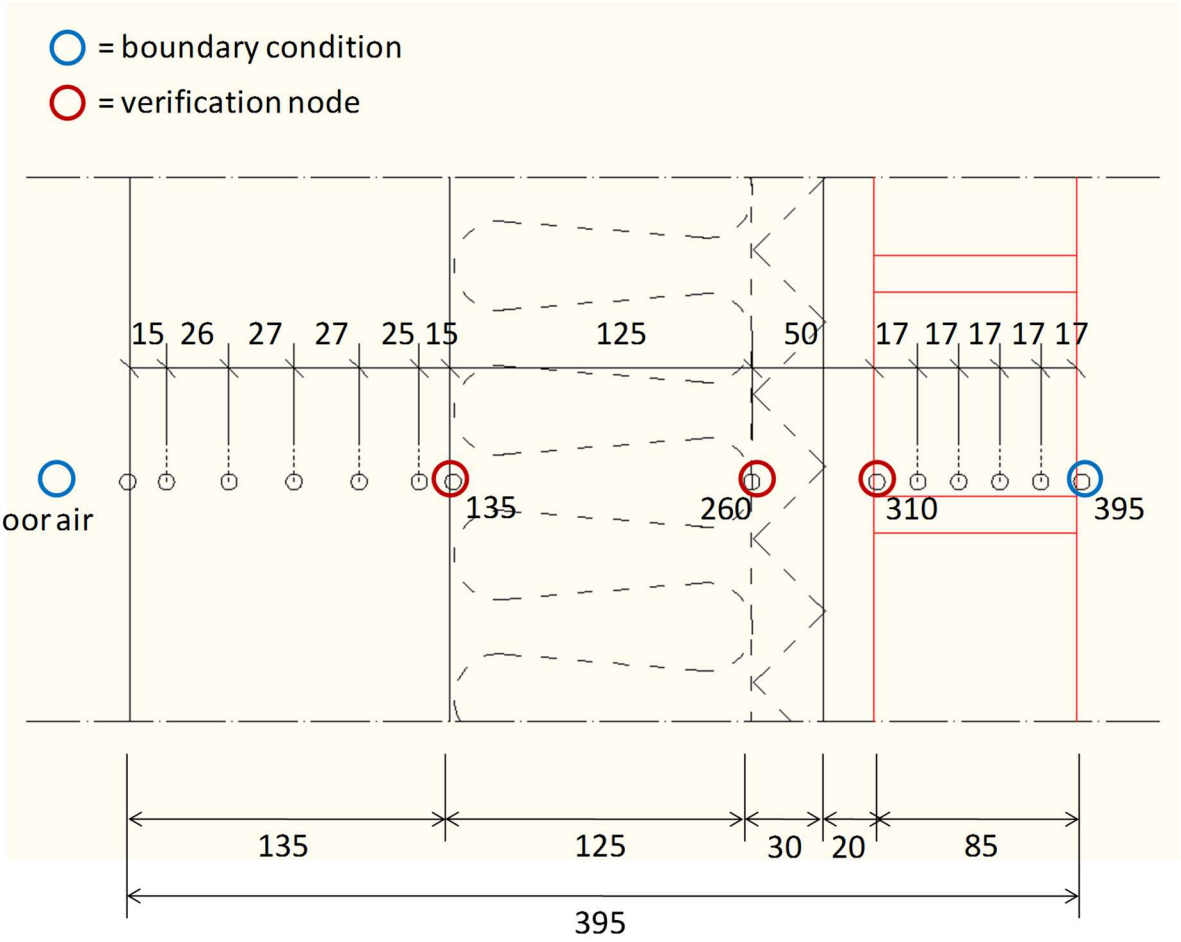

Fig. 2. Location of the 14 sensors inside the wall section.

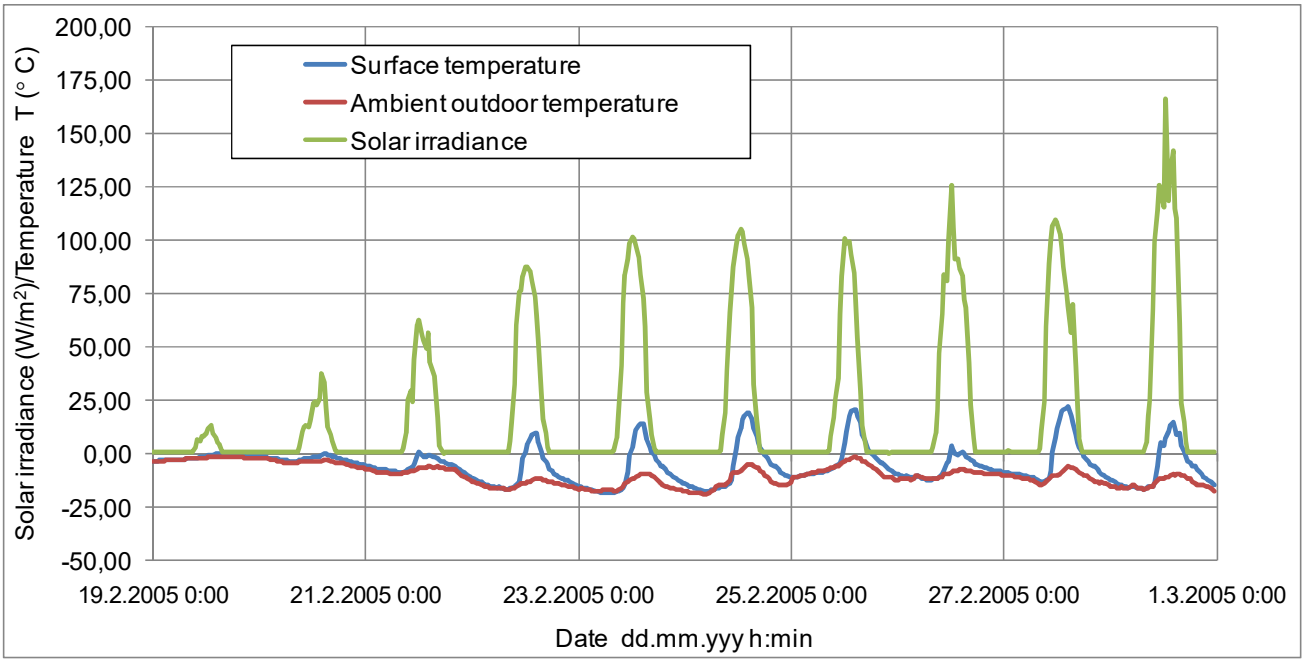

Fig. 3. Measured solar irradiation at the site, the ambient outdoor temperature and the measured outer surface temperature of brick leaf in late February 2005.

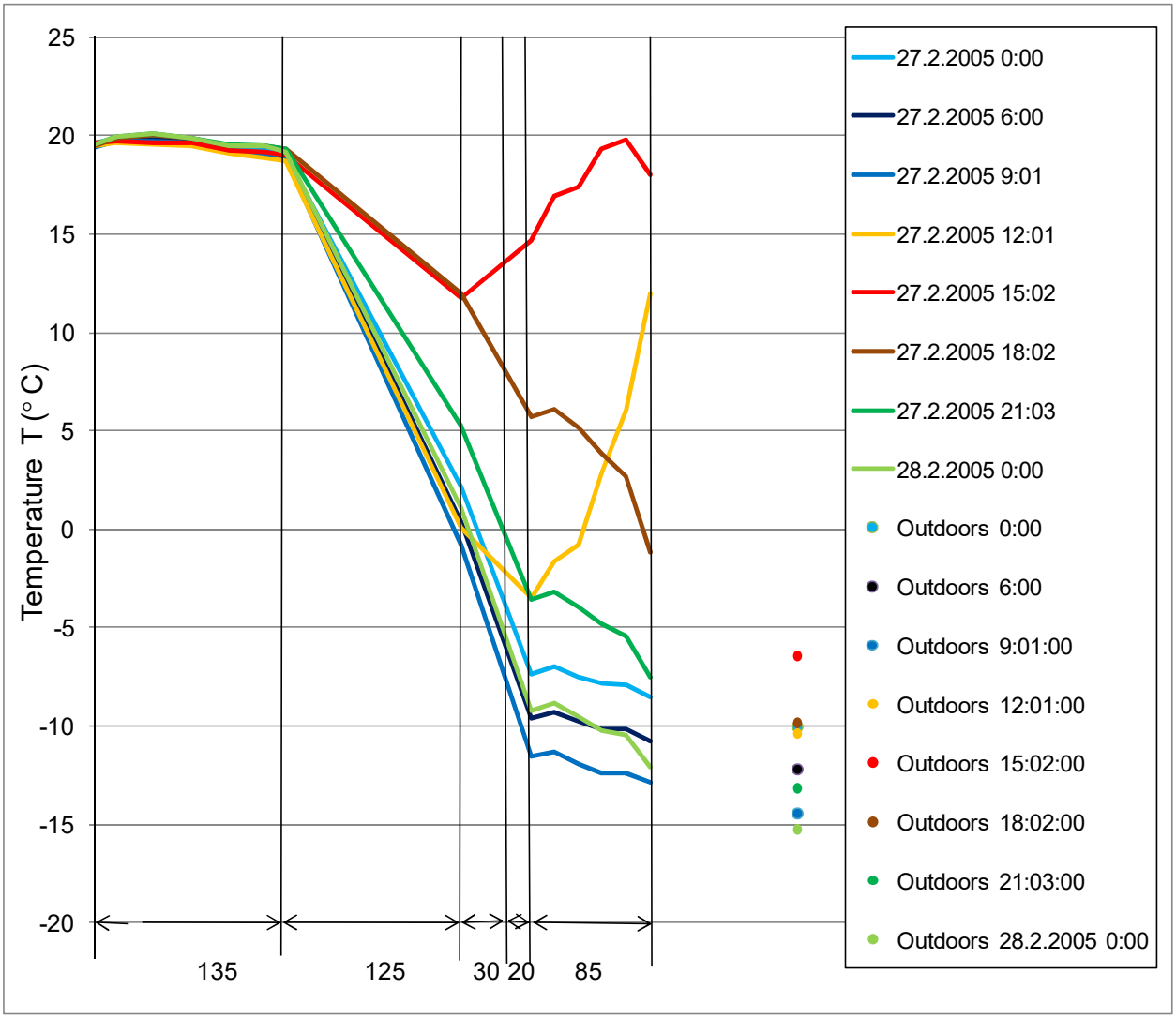

Fig. 4. Measured temperature distribution across the wall during 24 hrs period in late February 2005.

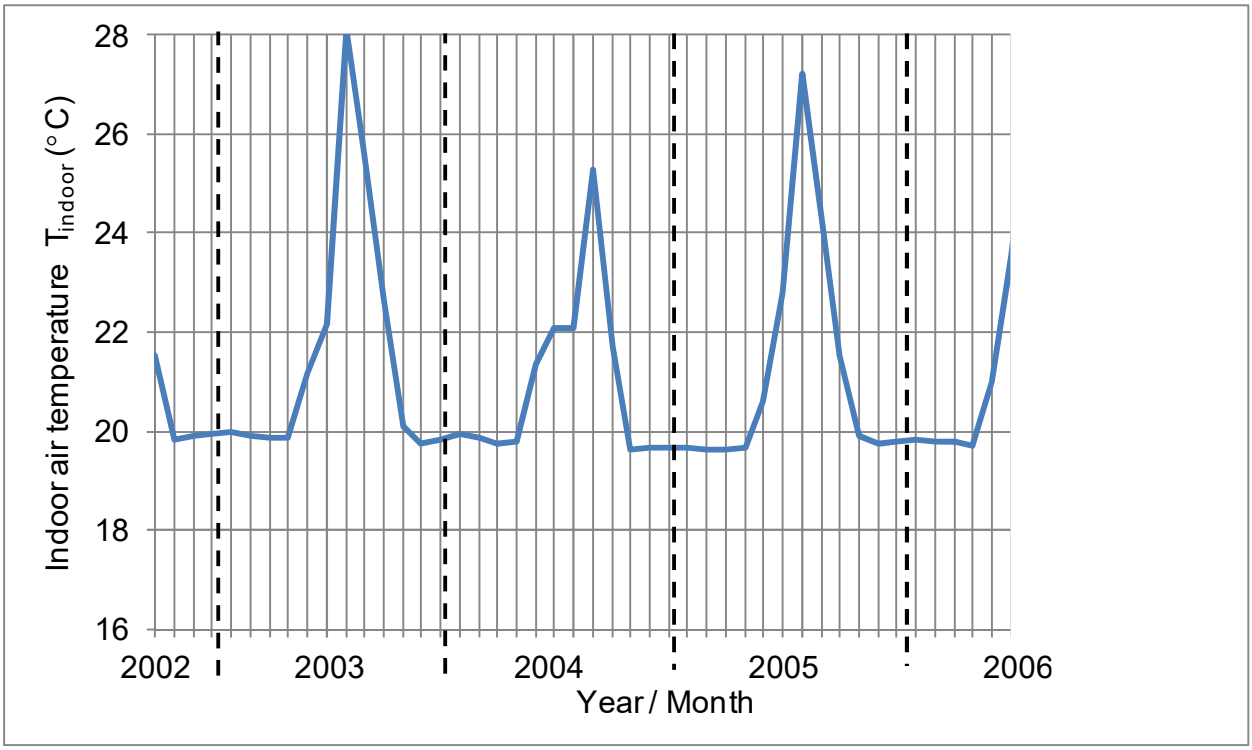

Fig. 5. Determination of the heating season from the measured indoor air temperatures.

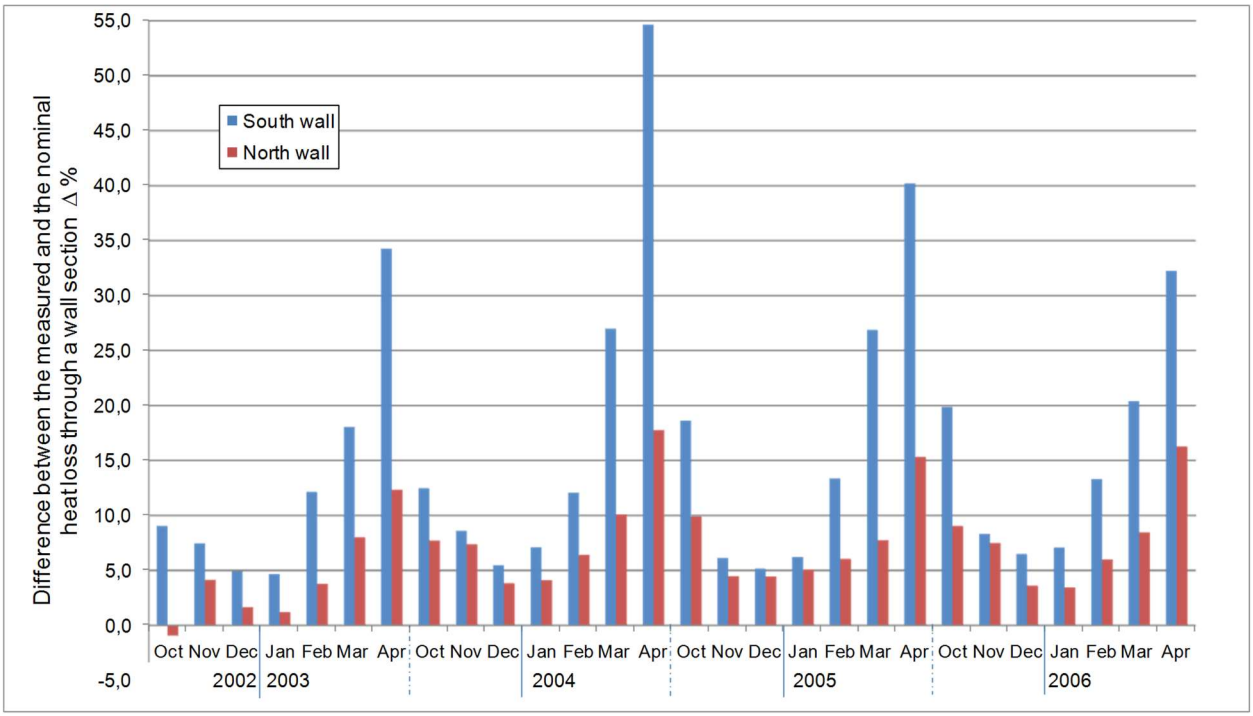

Fig. 6. Difference between the nominal calculated (method 1) and the measured (method 2) heat loss during the four heating seasons between 2002...2006.

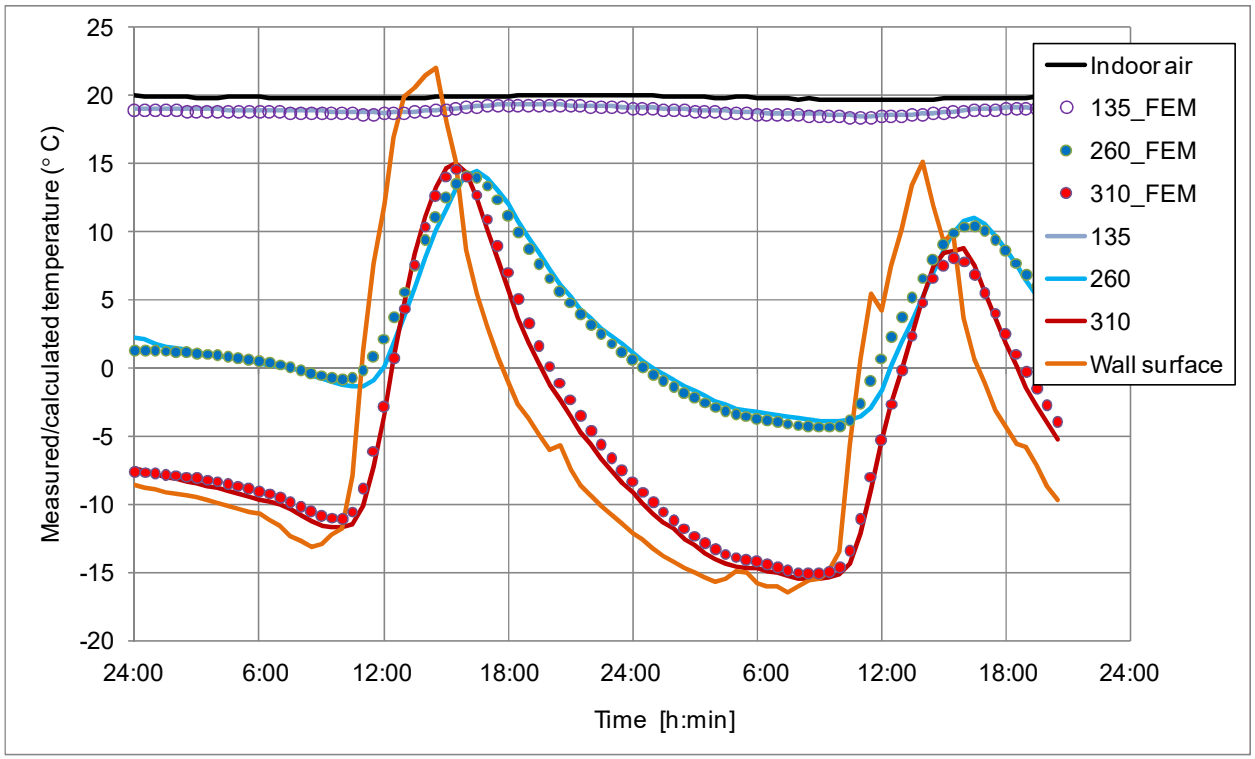

Fig. 7. Measured and calculated temperature changes inside the wall structure: outer surface of the load bearing brick wall (135), joint surface between mineral wool and wind shield board (260) and brickwork surface facing the air gap (310).

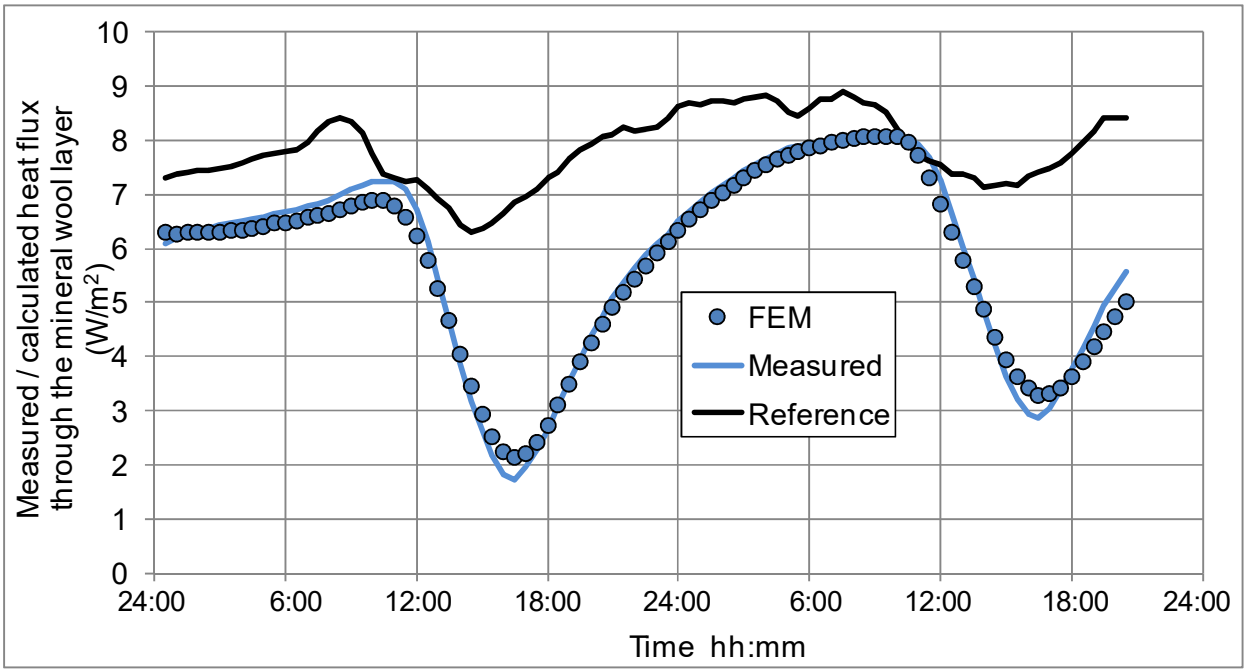

Fig. 8. Comparison between the measured and calculated actual heat flows (Measured, FEM) and the nominal flow (Reference) determined using the ambient indoor and outdoor temperatures.